BJ www.biochemj.org

BJ Structure

Biochem. J. (2012) **443**, 719–726 (Printed in Great Britain) doi:10.1042/BJ20111924

Toxic prefibrillar α-synuclein amyloid oligomers adopt a distinctive antiparallel β-sheet structure

María Soledad CELEJ*[1], Rabia SARROUKH†, Erik GOORMAGHTIGH†, Gerardo D. FIDELIO*, Jean-Marie RUYSSCHAERT† and Vincent RAUSSENS†

*Centro de Investigaciones en Química Biológica de Córdoba (CIQUIBIC, UNC-CONICET), Departamento de Química Biológica, Facultad de Ciencias Químicas, Universidad Nacional de Córdoba, Haya de la Torre y Medina Allende, Ciudad Universitaria, X5000HUA Córdoba, Argentina, and †Centre for Structural Biology and Bioinformatics, Laboratory for Structure and Function of Biological Membranes, Université Libre de Bruxelles, CP 206/2, Blvd. du Triomphe, B-1050 Brussels, Belgium

Parkinson's disease is an age-related movement disorder characterized by the presence in the mid-brain of amyloid deposits of the 140-amino-acid protein AS (α-synuclein). AS fibrillation follows a nucleation polymerization pathway involving diverse transient prefibrillar species varying in size and morphology. Similar to other neurodegenerative diseases, cytotoxicity is currently attributed to these prefibrillar species rather than to the insoluble aggregates. Nevertheless, the underlying molecular mechanisms responsible for cytotoxicity remain elusive and structural studies may contribute to the understanding of both the amyloid aggregation mechanism and oligomer-induced toxicity. It is already recognized that soluble oligomeric AS species adopt β-sheet structures that differ from those characterizing the fibrillar structure. In the present study we used ATR (attenuated total reflection)–FTIR (Fourier-transform infrared) spectroscopy, a technique especially sensitive to β-sheet structure, to get a deeper insight into the β-sheet organization within oligomers and fibrils. Careful spectral analysis revealed that AS oligomers adopt an antiparallel β-sheet structure, whereas fibrils adopt a parallel arrangement. The results are discussed in terms of regions of the protein involved in the early β-sheet interactions and the implications of such conformational arrangement for the pathogenicity associated with AS oligomers.

Key words: amyloidogenesis, amyloid oligomer, Parkinson's disease, secondary structure, structure–toxicity relationship, α-synuclein.

INTRODUCTION

In the so-called protein deposition diseases, specific proteins or peptides fail to adopt or remain in their native functional conformations and subsequently aggregate in amyloid fibrils with a canonical cross-β structure. These pathological conditions include well-known debilitating neurodegenerative disorders, such as Alzheimer's and Huntington's diseases and PD (Parkinson's disease) [1].

Accumulating evidence suggests that oligomeric intermediates, rather than final insoluble aggregates, are the primary toxic species [1]. Although the underlying molecular mechanism remains elusive, toxicity pathways have been associated with: (i) the establishment of aberrant protein interactions mediated by the exposure of flexible hydrophobic surfaces [1,2]; (ii) the propagation of folding defects by interfering with protein quality control and clearance mechanisms [2,3]; and (iii) the impairment of biomembranes [1,4]. These different patterns of phatobiology are not mutually exclusive and may operate simultaneously. It appears that oligomer-induced toxicity is related to their structure rather than to their sequence, since prefibrillar aggregates comprising non-disease-related proteins showed similar toxicity in cell culture [5]. Besides, a variety of prefibrillar oligomers share common structural epitopes [6] and toxicity of such species seems to also correlate with the accessibility of ANS (1-anilinonaphthalene 8-sulfonate)-binding hydrophobic patches [2,7,8].

PD is an age-related movement disorder affecting more than 2% of the population over 65. PD is associated with a dying back of axons projecting from the SNpC (substantia nigra pars compacta) to the striatum, culminating in a massive loss of dopaminergic neurons in the SNpC. The histopathological hallmark of PD is the presence of fibrillar intraneuronal proteinacious inclusions, termed Lewy bodies, the main component of which is the 140-amino-acid presynaptic protein AS (α-synuclein), whose normal function remains unclear. Growing evidence suggests a link between misfolded AS and the pathogenesis of PD as well as several other related disorders [9].

Structurally, recombinant human AS is a natively unfolded monomer [10], with transient long-range domain interactions stabilizing a closed conformation [11]. In the fibrillar form, the monomers adopt a parallel in-register structure, with a β-sheet-rich core region spanning residues 38–95, from which the two termini are excluded [12–14]. A model for the fold of AS fibrils has been proposed [15]. Fibrillation of AS follows a nucleation polymerization pathway involving major structural rearrangements and the population of diverse transient prefibrillar species varying in size and morphology [16,17].

Compelling evidence points to AS oligomers being the most neurotoxic species. It has been demonstrated that AS oligomers disrupt membranes [18–21] and cause cell death *in vitro* [22,23] and in animal models [24,25]. Additionally, certain AS aggregates may be involved in the prion-like cell-to-cell spreading of the PD pathology [26].

Despite their relevance in neurodegeneration and disease, structural information about oligomeric AS is still limited. Several technical limitations arise from the transient [17] and heterogeneous [23,27] nature of oligomeric intermediates,

Abbreviations used: Aβ, amyloid-β peptide; AS, α-synuclein; ATR, attenuated total reflection; AVD, avidin; ConA, concanavalin A; FTIR, Fourier-transform infrared; NAC, non-Aβ component; PD, Parkinson's disease; SNpC, substantia nigra pars compacta; TBST, TBS/Tween 20; TEM, transmission electron microscopy; ThioT, thioflavin T; TPI, triose phosphate isomerase.

[1] To whom correspondence should be addressed (email mcelej@mail.fcq.unc.edu.ar).

and the low yield in which they can be produced [18]. CD and IR spectroscopies indicated that AS oligomeric intermediates contain substantial β-sheet structure [18,28–30], although some α-helical contribution has also been observed by Raman spectroscopy [31]. Also, ^{13}C cross-polarization solid-state NMR studies revealed that AS oligomers obtained by cold-assisted dissociation of fibrils have non-fibrillar β-sheet structure [21]. In addition, fluorescence measurements on engineered tryptophan AS variants showed that residues in the N-terminal and central part of the protein (towards at least residue $\sim$90) comprise the core of oligomeric AS, the C-terminal part being the most solvent-exposed region [32].

In the present study, we used ATR (attenuated total reflection)–FTIR (Fourier-transform infrared) to gain insights into the structure of AS oligomers. Unlike the above-mentioned structural studies, we were able to discriminate between the β-sheet organization within oligomers and fibrils. We demonstrate that AS oligomers adopt an antiparallel β-sheet structure, as opposed to the parallel arrangement present in fibrils. We discuss possible regions that may be involved in such early β-sheet interactions. As previously shown for oligomeric Aβ (amyloid-β peptide), a peptide linked to Alzheimer's disease [33], AS oligomers adopt an antiparallel β-sheet structure that might represent a distinctive signature of amyloid oligomers.

EXPERIMENTAL

Protein expression and purification

Recombinant human AS was expressed in *Escherichia coli* BL21(D3) cells transformed with a pT7-7 plasmid encoding for the protein. Bacterial cultures were incubated at 37 °C in LB (Luria–Bertani) broth containing ampicillin (100 mg/ml). At $D_{600} = 0.7$, cells were induced with 0.5 mM IPTG (isopropyl β-D-thiogalactopyranoside), cultured at 37 °C for 4 h and centrifuged at 4000 ***g*** for 15 min. The pellet was resuspended in 10 mM Tris/HCl, pH 8.0, 1 mM EDTA and 1 mM PMSF, and lysed by three freeze-thaw cycles and sonication (duty cycle 70, output control 5, 25 °C on a Branson Sonifier 250). The cell suspension was boiled for 30 min and centrifuged at 13000 ***g***. Streptomycin sulfate (10 mg/ml) was added to the supernatant, and the mixture was stirred for 15 min at 4 °C and centrifuged as above. Upon addition of ammonium sulfate (360 mg/ml) to the supernatant, the solution was stirred for 15 min at 4 °C and centrifuged as above. The pellet was resuspended in 25 mM Tris/HCl, pH 7.7, loaded on to a POROS HQ (Applied Biosystems) column on an Äkta purifier (GE Healthcare), and eluted with a 0–600 mM NaCl salt gradient. The pure AS (assessed by SDS/PAGE) was dialysed overnight against Milli-Q water or 10 mM Hepes, pH 7.4, and 0.02 % sodium azide, freeze-dried when needed, and stored at − 20 °C.

Preparation of monomeric and aggregated AS

Monomeric AS stock solutions were prepared in 10 mM Hepes, pH 7.4, and 0.02 % sodium azide and centrifuged (14100 ***g***, 30 min) before use in order to remove possible aggregates. Protein concentration was determined by absorbance using an ε_{275} of 5600 $M^{-1} \cdot cm^{-1}$.

Oligomerization protocols were adapted from previous studies [18,30,31]. Monomeric AS stock solutions (250 μM) in 10 mM Hepes, pH 7.4, were freeze-dried and redissolved using Milli-Q water at a concentration of 1 mM, and then incubated for 19 h in a Thermomixer5436 (Eppendorf) at 25 °C and 800 rev./min (this oligomeric preparation will be referred to as condition O-I for the rest of the paper). The samples were centrifuged (14100 ***g***, 30 min) and filtered through a 0.22 μm-pore-size filter to remove possible extremely high-molecular-mass species. Oligomeric AS was separated from the monomer using an Amicon Ultra-0.5 100 kDa cut-off filter (Millipore). Diafiltration was repeated until no monomer was detected by native gradient PAGE. Alternatively, freeze-dried AS from Milli-Q water was dissolved in 10 mM Hepes, pH 7.4 (condition O-II), and oligomeric species were purified as described above.

Fibrillation was achieved by incubating 400 μM monomeric AS stock solutions in glass vials (Zinsser Analytik) at 37 °C (Dalvo incubator) with constant stirring at 350 rev./min (Telesystem 15.20, Variomag) using Teflon magnetic microbars (Roth) (condition F-I). Alternatively, AS solutions were incubated at 70 °C and 800 rev./min in a Thermomixer5436 (Eppendorf), conditions that lead to faster aggregation kinetics [34] (condition F-II). Fibril formation was monitored using the ThioT (thioflavin T) fluorescence assay. Fibrils were isolated by three consecutive cycles of centrifugation (14000 ***g***, 30 min) and resuspended in 10 mM Hepes buffer. Protein concentrations in monomeric units were determined by the absorbance of aliquots incubated in 6 M guanidinium chloride at 25 °C for 24 h.

Dot blot

Monomeric, oligomeric or fibrillar AS (2 μg) were spotted on to a nitrocellulose membrane and fixed for 10 min with 10 % (v/v) acetic acid and 25 % (v/v) propan-2-ol. After blocking for 1 h with 10 % (w/v) non-fat dried skimmed milk powder in 0.01 % TBST (TBS/Tween 20; 10 mM Tris/HCl, pH 8, 150 mM NaCl and 0.01% Tween 20) and washing, the membranes were incubated with either a mouse anti-AS antibody (Sigma) for 3 h at 25 °C (1:4000) or a rabbit anti-oligomer A11 antibody (Millipore) overnight at 4 °C (1:3000), both in 5 % (w/v) non-fat dried skimmed milk powder and 0.01 % TBST. After washing three times with 0.01 % TBST and once with PBS, blots were probed with either IRDye 800CW anti-mouse IgG or IRDye 800CW anti-rabbit IgG (both from Li-Cor Biosciences) and scanned using an Odyssey infrared scanner (Li-Cor Biosciences).

Native gradient PAGE

Native polyacrylamide gels were cast with a linear gradient from 4 to 15 %. HMW Native Marker (GE Healthcare) was loaded as a molecular mass marker. Electrophoresis was performed under non-denaturing conditions at a constant 80 V. Gels were stained with silver nitrate.

ThioT fluorescence assay

Corrected emission spectra were acquired with a Cary Eclipse spectrofluorimeter (Agilent Technologies), using excitation at 446 nm, spectral bandwidths of 10 nm and a 1 cm path cuvette. Experiments were performed at 25 °C using final concentrations of 0.25 μM protein and 5 μM dye.

Seeding aggregation assay

The aggregation of AS was carried out in 25 mM Tris/HCl, pH 7.4, and 150 mM NaCl. The protein was filtered through a 100 kDa cut-off filter (Amicon Ultra-0.5, Millipore) and aliquots of 350 μl were incubated as described previously for fibrillation condition F-I. For seeding experiments, oligomers O-I and O-II and fibrils F-I were prepared as described above. Aggregation reactions were seeded with purified oligomers O-I, O-II or sonicated fibrils (5 min in a bath sonicator at 25 °C), at a final

concentration of 8 μM (oligomer seeds) or 3 μM (fibrillar seeds). In all cases, the total protein concentration was kept at 108 μM in terms of monomeric units. The extent of aggregation was monitored by the ThioT fluorescence assay as described above. A total of two to four replicates were run independently. The results were averaged and normalized to the averaged final values obtained after curve fitting.

TEM (transmission electron microscopy)

Aggregated AS (5 μl) was adsorbed on to Formvar-coated carbon grids (200 mesh). Grids were washed with Milli-Q water and stained with 1 % (w/v) uranyl acetate. The samples were imaged in a JEM-1200 Ex (Jeol) transmission electron microscope equipped with a GATAN camera, model 785.

ATR–FTIR

IR spectra were recorded on an Equinox 55 IR spectrophotometer (Bruker Optics) equipped with a single reflection diamond reflectance accessory (Golden Gate, Specac). The spectrometer was continuously purged with dried air. A total of 256 accumulations were performed to improve the signal/noise ratio. Spectra were recorded at 21 °C using a resolution of 2 cm^{-1}. The sample (1.5–5 μl) was spread on the diamond crystal surface and excess water was removed under nitrogen flow. The protein films were rehydrated using nitrogen saturated in ^2H_2O to obtain deuterated protein spectra.

Secondary structure analysis

The water vapour and side chain contributions were subtracted and then the spectra were baseline corrected and normalized for equal area between 1700 and 1500 cm^{-1}. All spectra were deconvoluted using a Lorentzian deconvolution factor with a full width at the half maximum of 20 cm^{-1} and a Gaussian apodization factor with a full width at the half maximum of 13.33 cm^{-1} to obtain a resolution enhancement factor $K = 1.5$. The bands identified in the deconvolved spectra were used for curve fitting of the deuterated original ($K = 1$) spectra using Gaussian/Lorentzian bands [35].

β-Sheet organizational index

For comparative analysis, FTIR spectra of well-known β-sheet proteins were extracted from the RASP50 database [36]: AVD (avidin) from hen egg white, ConA (concanavalin A) from jack bean and TPI (triose phosphate isomerase) from *Saccharomyces cerevisiae*. FTIR spectra of bacterial outer membrane porin (OmpF), as well as oligomers (oAβ) and fibrils (fAβ) from Aβ(1–42) were described in a previous study [33]. The Aβ peptide was incubated at 4 °C in 20 mM TBS, pH 7.4, and 100 mM NaCl over 24 h for oligomerization or at room temperature in 0.5 mM Hepes, pH 7.4, over 36 days for fibrillation [33]. For the sake of comparison, all baseline corrected, non-deuterated and self-deconvoluted (using the same deconvolution parameters as described above) spectra were fitted using the same eight band components (these bands were centred, before fitting, respectively at 1695, 1683, 1678, 1664, 1657, 1653, 1640 and 1624 cm^{-1}). Then, the so-called 'β-sheet organizational index', allowing differentiation between the parallel and antiparallel β-sheet, was defined as the quotient between the intensity of the fitted bands assigned to the high and low wavenumber β-sheet components at their corresponding final (after fitting) positions. For the different spectra, the final position of the high wavenumber β-sheet component was located between 1693 and 1697 cm^{-1}, and for the low wavenumber component, the final position varied between 1624 and 1632 cm^{-1} (with the exception of TPI, which was at 1641 cm^{-1}, refer to [35,36] and references therein for details).

RESULTS AND DISCUSSION

Elucidating the conformational organization of oligomeric AS is fundamental for understanding the amyloid aggregation mechanism and oligomer-induced cell toxicity. It is already recognized that soluble oligomeric AS species contain β-sheet structural elements [18,30,31] that may differ from the typical fibrillar structure [21,31]. In the present study, we used ATR–FTIR, a technique especially sensitive to β-sheet structure, to unravel the structural signature of AS oligomers.

Oligomer characterization

Several methods for producing stable AS oligomers have been reported [18,21–23,30,31]. We used freeze-drying and high protein concentration as a simple method to induce oligomerization. This approach results in β-sheet oligomers that exhibit vesicle disruption properties [18,30,31]. Since different conditions could lead to structurally and functionally different oligomeric species, we employed five complementary techniques to characterize the oligomers produced.

The purity of the oligomeric preparations after diafiltration was assessed by native PAGE electrophoresis (Figure 1A). Since the migration of a protein in this system depends on its mass, charge and conformation, the assignment of a correct molecular mass is rather difficult. However, we could conclude that oligomeric AS, observed as broad high-molecular-mass bands (Figure 1A, lines 3 and 4) near the ferritin band (~440 kDa, Figure 1A, line 1), did not contain monomeric protein (Figure 1A, line 2). A similar electrophoretic pattern was reported previously [30]. Moreover, the smeared oligomeric bands indicated that these samples contain a broad size distribution of protein aggregates.

The morphology of the aggregates was appraised by electron microscopy. Fibrillar AS samples were unbranched and several micrometres long, with widths of 6–10 nm (Figure 1B, bottom panel) as expected for mature amyloid fibrils [12]. The same morphological features were observed for fibrils prepared at 70 °C (results not shown), as reported previously [34]. On the other hand, the purified oligomers appeared as spheroidal, polydisperse species with sizes in the range 10–60 nm (Figure 1B, top and middle panels), in agreement with PAGE data (Figure 1A). Importantly, no fibrillar aggregates were observed in these preparations.

Furthermore, neither oligomeric nor monomeric AS enhanced ThioT fluorescence (Figure 1C), a sensitive amyloid dye that exhibits significant changes in fluorescence upon intercalation into the fibrillar core. As expected, ThioT became highly fluorescent in the presence of AS fibrils (Figure 1C). Since there is no evidence of the presence of fibrillar material in the oligomeric samples, these results suggest that the produced AS oligomers lack the stacked in-register β-sheet structure distinctive for amyloid fibrils. This fact correlates with previous findings that soluble on-pathway oligomers have a non-fibrillar β-sheet structure [21].

Moreover, the oligomeric species were recognized by the A11 antibody (Figure 1D), a conformation-specific antibody targeting oligomeric assemblies of many amyloidogenic proteins [6]. Conversely, neither the monomer nor the fibrils showed

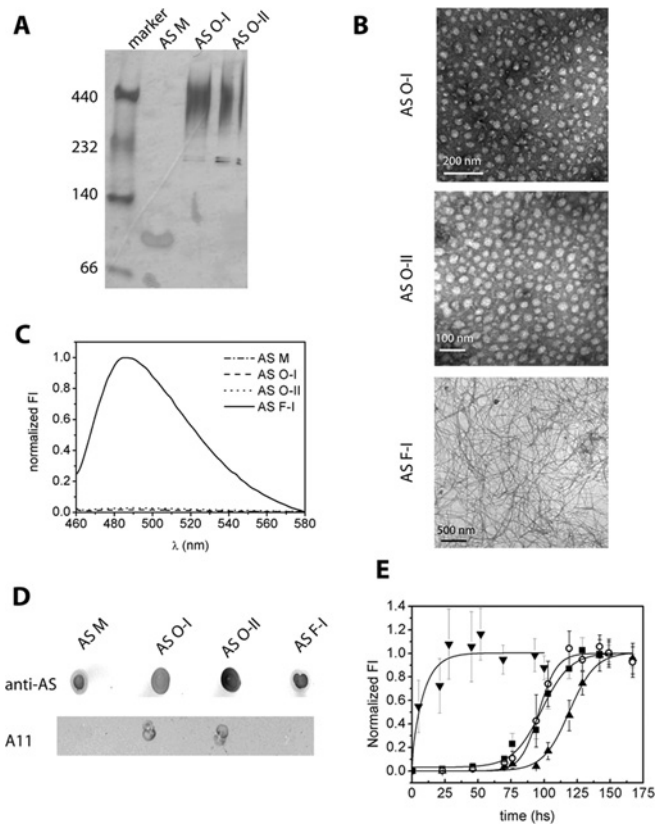

Figure 1 Characterization of AS oligomers

(**A**) Native gradient PAGE with a polyacrylamide gradient from 4 to 15 % stained with silver nitrate. marker, native molecular marker (ferritin, 440 kDa; catalase, 232 kDa; lactate dehydrogenase, 140 kDa; and BSA, 66 kDa); AS M, monomeric AS; and AS O-I and AS O-II, oligomeric AS obtained under oligomer-forming conditions O-I and O-II respectively. (**B**) TEM images of uranyl-acetate-stained AS oligomers self-assembled under oligomer-forming conditions O-I (top panel) and O-II (middle panel), and AS fibrils formed under fibril-forming condition F-I (bottom panel). (**C**) Fluorescence emission spectra of ThioT in the presence of AS monomer (-·-·-), oligomers (oligomerization condition O-I, - -, and O-II, · · ·) and fibrils (fibrillation condition F-I, continuous line). (**D**) Immunobloting with anti-AS and the A11 anti-oligomer antibody against the same samples detailed in (**C**). (**E**) Kinetics of AS aggregation monitored by ThioT fluorescence in the absence (▲) and the presence of oligomer seeds (oligomerization condition O-I, ○, and O-II, ■) and fibrillar seeds (▼).

significant reactivity against A11 (Figure 1D). This indicates that the oligomers produced share conformational features with other toxic prefibrillar intermediates [6].

Finally, we tested whether the oligomeric species were able to seed amyloid AS formation. Monomeric AS showed the characteristic sigmoidal ThioT profile (Figure 1E), as expected for a nucleation-polymerization process [16]. The time point of 50 % apparent conversion ($t_{1/2}$) was approximately 118 h. Consistent with this model [16], sonicated fibrils bypassed the lag-phase and caused rapid aggregation ($t_{1/2} = \sim 5.5$ h, Figure 1E). Addition of oligomers O-I or O-II shortened the lag-phase for nucleation, yielding an aggregation half-time of $\sim$97 h (Figure 1E). This observation indicates that the oligomers produced are on-pathway intermediates.

Overall, we conclude that the isolated AS oligomers are on-pathway intermediates that share the same structural motif as other prefibrillar oligomers and that they do not possess the canonical cross-β-fibril structure.

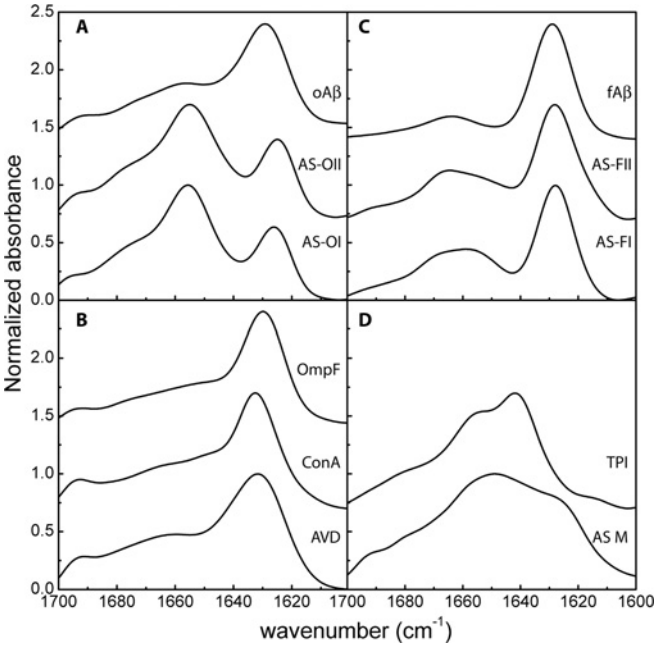

Figure 2 Secondary structural features of AS oligomers and fibrils assessed by ATR–FTIR

Normalized FTIR spectra in the amide I region of (**A**) AS oligomers formed under oligomer-forming condition O-I, AS oligomers formed under oligomer-forming condition O-II and oligomeric Aβ (oAβ); (**B**) the three selected antiparallel β-sheet proteins AVD, ConA and OmpF; (**C**) AS fibrils formed under fibril-forming condition F-I, AS fibrils formed under fibril-forming condition F-II and fibrillar Aβ (fAβ); (**D**) monomeric AS (AS M) and the parallel β-sheet protein TPI. All spectra were deconvoluted with a resolution enhancement factor $K = 1.5$ and shifted for better visualization.

Secondary structural features of distinct AS species

IR spectroscopy has proven useful to discriminate between parallel and antiparallel β-sheets, since the former shows a major band component at $\sim$1640–1630 cm^{-1}, whereas the latter displays a major band at $\sim$1630 cm^{-1} and an additional approximately 5-fold weaker band at $\sim$1695 cm^{-1} [35,37,38].

The FTIR absorbance spectra showed distinctive features depending on the aggregation state of the protein (Figure 2). The spectrum of the monomeric protein was centred at 1650 cm^{-1}, as expected for a substantially unfolded protein (Figure 2D). The most striking feature of the amide I absorption band of AS in the two oligomer-forming conditions was the presence of a band at 1625 cm^{-1} along with a prominent shoulder at 1695 cm^{-1} (Figure 2A), the two characteristic components of an antiparallel β-sheet structure. However, these features were absent in the FTIR spectra of AS in the two fibril-forming conditions, which displayed the typical parallel β-sheet features characterized by a maximum at 1628 cm^{-1} (Figure 2C). These data clearly indicate that fibrillar and prefibrillar aggregated amyloid species adopt different structures, in agreement with recent NMR data reporting on the non-fibrillar β-sheet nature of AS oligomers [21]. This band assignment became unambiguously clear when we compared the FTIR profiles of AS aggregated species with those of well-known β-sheet-rich proteins, along with oligomeric and fibrilar Aβ amyloid aggregates. First, AS oligomers were compared with oligomeric Aβ (Figure 2A) as well as other antiparallel β-sheet proteins, namely AVD, ConA and OmpF (Figure 2B), which correspond respectively to the following architecture/topology: β-barrel/Lipocalin, β-sandwich/Jelly Roll and β-barrel/Porin, according to the CATH nomenclature. Secondly, AS fibrils were

compared with fibrillar Aβ (Figure 2C) and to the parallel β-sheet protein TPI (Figure 2D), which is classified as an α/β-barrel/TIM barrel protein according to the CATH nomenclature. The visual inspection of the FTIR profiles shown in Figure 2 clearly confirms the different β-strand orientation adopted by AS in the oligomeric and fibrillar forms. A baicalein-stabilized AS oligomer FTIR spectrum has been published previously [28]. We could notice that it presented the two characteristic IR components of antiparallel β-sheets, although this structural conformation was not suggested by the authors. In addition, similar spectral features were observed for oligomers formed by Aβ(1–40) [39,40], a prion-related peptide [41] and β2-microglobulin [42]. On the basis of our results (the present study and [33]) and the examples cited above, we postulate that an antiparallel β-sheet organization might represent a common structural motif in amyloid oligomers.

In order to estimate the secondary structure content of each species, we performed a quantitative analysis of the amide I region on deuterated samples by self-Fourier deconvolution followed by curve-fitting. The β-sheet content was lower than 8 % in AS monomers and increased up to approximately 26 % in AS oligomers and ~51 % in AS fibrils, in good agreement with previous results obtained by vibrational spectroscopy [28,31]. The progressive increase in β-sheet content was accompanied by a concomitant decrease in random coil and/or helical contribution (observed absorbance 1650–1660 cm^{-1}) from ~60 % in monomers to 52 % in oligomers and 27 % in fibrils. In both aggregated species, the β-turn content (~1670 cm^{-1}) was approximately 22 %. The estimates of secondary structure in AS fibrils correlated with EPR and NMR data that revealed a folded region (residues ~34–101) containing extended stretches of β-strands along with loops or turns, from which the two termini protrude [13–15], whereas the N-terminus exhibits static disorder from at least residue 22 onward, the C-terminus, starting from at least residue 107, is unstructured and mobile [14].

Although the accuracy of the determination of secondary structure composition is prone to some error, the amide I profiles of AS oligomers and fibrils unequivocally indicate a change in the proportion and quality of the β-structures (Figure 2). The 1695/1630 cm^{-1} intensity ratio can be considered as proportional to the percentage of antiparallel arrangement of β-strands in β-sheets [38]. Since the precise positions of the β-sheet band components depend on the number, length and twisting of the strands [35] (see, for example, the upshifted spectrum for TPI in Figure 2D), we defined the 'β-sheet organizational index' as the intensity ratio of the corresponding high and low wavenumber regions assigned to β-sheets (see the Experimental section). The calculated values for this index for the samples studied included in Figure 2 are depicted in Figure 3. The β-sheet organizational indexes for AS oligomers were high and close to those calculated for the three selected mainly β proteins (Figure 3), whose β-strands are clearly arranged in an almost complete antiparallel fashion. This suggests that 100 % of the β-strands in AS oligomers also adopt an antiparallel conformation, similar to what was found for Aβ oligomers [33,40]. In contrast, the corresponding indexes for both types of AS fibrils were low and similar to the values determined for TPI and Aβ fibrils, which are folded in parallel β-sheet structures, in perfect agreement with the EPR results reporting on the parallel in-register AS fibril conformation [13].

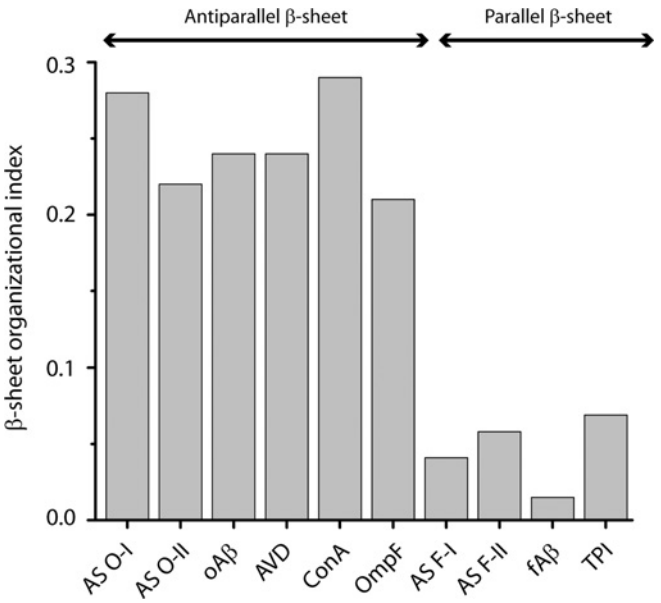

Figure 3 β-Sheet organizational index of AS oligomers and fibrils

Intensity ratio between the high and low wavenumber β-sheet components for AS and Aβ amyloid aggregates and representative proteins as detailed in Figure 2 (see the Experimental section for details).

The β-sheet antiparallel oligomer organization in the context of current knowledge on AS

Three functional domains are distinguished in the AS sequence (Figure 4A): (i) the amphipatic N-terminus (residues 1–60), which bears the three genetic mutations linked to early onset of PD; (ii) the central hydrophobic region (residues 61–95) known as the NAC (non-Aβ component); and (iii) the highly acidic C-terminus (residues 96–140) that modulates fibril formation. In the monomeric state, the C-terminus folds back on to the central hydrophobic region of the protein, establishing long-range interactions that prevent aggregation [11]. On the basis of a number of NMR determinations, five β-strands (namely β1–β5, encompassing residues 37–43, 52–59, 62–66, 68–77 and 90–95 respectively, Figure 4B) have been assigned to the AS fibril core [15]. Intramolecular interactions between the consecutive β-strands would contribute to the formation of the five-layered β-sandwich that gives rise through intermolecular interactions to the parallel in-register β-sheet fibril structure [15] (Figure 4C). The sequence encompassing β3–β5 corresponds to the amyloidogenic NAC region (Figure 4B). Indeed, the contiguous β3–β4 stretch bears the highest predicted β-sheet [43] and aggregation [44] propensities. In addition, β4 overlaps with the span of 12 residues (from Val^{71} to Val^{82}) identified as a key element for the assembly of the protein into fibrils [45].

Fluorescence determinations on a number of engineered tryptophan AS variants revealed that the region spanning residues from at least 4 to 90 comprise the solvent-protected area in the oligomeric state [32]. However, the exact regions involved in β-sheet interactions are unknown. Since β3 and β4 are prone to aggregate and, upon fibrillation, they are located in the centre of the fibril, we could expect them to form stable parallel β-sheets. In addition, bearing in mind that the release of long-range interactions constitutes a pre-requisite to trigger fibrillation [11], we speculate that regions in the protein involved in nucleation and early stages of oligomerization may differ from those that constitute the inner core of the fibrils. In order to prompt aggregation and allow reorganization of the β-sheet network, these regions should display propensity to establish inter-molecular β-sheet interactions and, more likely, be located in the periphery of the AS fibril. Both β1 and β5 would fulfill such criteria [15,43,44]. Since β5 is highly shielded by

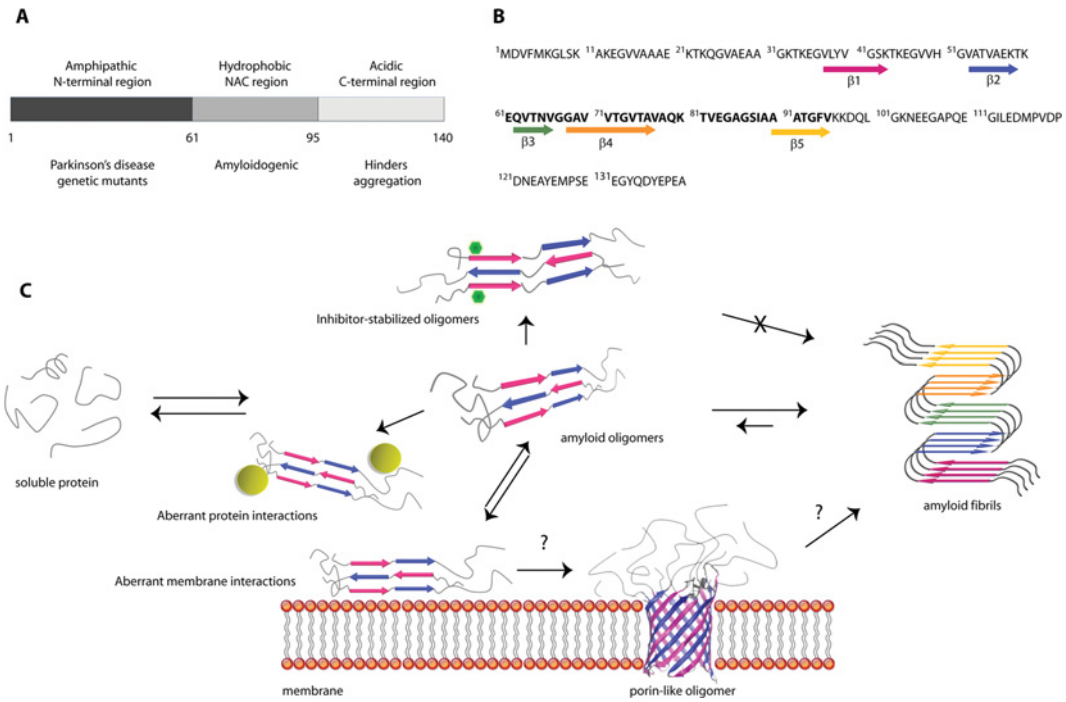

Figure 4 Schematic representation of AS primary sequence, self-assembly and toxicity

(**A**) AS functional domains. The N-terminal amphipathic region contains the three point mutations linked to autosomal dominant early-onset PD. The central NAC region encompasses the most hydrophobic residues and promotes aggregation. The C-terminal portion modulates aggregation. (**B**) β-Strand localization in the core fibrillar region according to [15]. The NAC region is represented in bold type. (**C**) Schematic representation of AS aggregation and oligomer-induced toxicity. A significant rearrangement of the protein structure, involving the population of oligomeric species, occurs during fibrillogenesis. Whereas amyloid fibrils are folded in a parallel in-register β-sheet structure, β-strands in AS oligomers are arranged in an antiparallel fashion. Oligomeric species may be trapped by small molecules (green hexagons) that preferentially target regions encompassing residues ~3–23 and/or 38–51 and inhibit fibril formation. Oligomers may expose hydrophobic regions that can mediate aberrant interactions with multifunctional proteins (yellow circles), leading to the collapse of essential cellular functions. As another possible co-existent mechanism, amyloid oligomers can compromise the integrity of membranes, probably through their antiparallel β-sheet-structured regions.

interactions with the C-terminus [11], we postulate that the region enclosing β1 is probably involved in early β-sheet interactions. In this context, we note that several small-molecule inhibitors of fibrillogenesis preferentially interact with regions encompassing residues ~3–23 and/or 38–51 [46–48], where Tyr^{39} plays a major role in anchoring the anti-amyloid compounds [47,48]. Interestingly, some of these inhibitors trap AS oligomers that do display β-sheet structure to some extent [28,48]. Thus they seem to bias the structural ensemble in a fashion that constrains β-sheet elongation and reorientation. In addition, a Trp^{39} AS variant was sensitive to the build-up of oligomers formed during the lag-phase of fibrillation [49]. Finally, fluorescence resonance energy transfer measurements between Tyr^{39} and Trp^{125} pointed to conformational differences between oligomers populated at different stages of aggregation [29]. Taken together, these results speak in favour of the key role of the β1 region in the early steps of AS amyloid formation. In addition, to account for the percentage of β-structure content estimated from fitting analysis, other regions of the protein must participate in such a structural arrangement. It has been shown recently that disruption of potential specific salt bridges in adjacent regions to β1 and β2 led to the formation of oligomers which were highly toxic *in vivo* [25]. Thus one could expect β2 to also be involved in these oligomeric β-sheet interactions.

The inherent cytotoxicity of oligomers was postulated to be a general phenomenon related to their structure [5]. Major efforts are currently being directed at unravelling the structural basis of gain-of-function toxicity associated with amyloid oligomers, and mounting evidence suggests that they share structural similarities that would underlie their common pathways of pathobiology [7,22]. For instance, it has been proposed that the exposure of hydrophobic surfaces [7,8] would endow oligomers with the ability to engage in aberrant interactions with multifunctional proteins leading to the collapse of essential cellular functions [2]. In this regard, the higher proportion of random/helical structures found in AS oligomers as compared with fibrils speaks in favour of such mechanism and correlates with the higher toxicity associated with the prefibrillar intermediates.

On the other hand, several reports indicate that AS oligomers compromise the integrity of membranes both *in vitro* and *in vivo* [18,21,23,25,30]. The molecular bases of such effects are still a matter of debate and diverse mechanistic models, i.e. pore formation, membrane thinning and lipid extraction, have been proposed (recently reviewed in [4]). On the basis of our findings that AS oligomers adopt an antiparallel β-sheet conformation, a structural feature also present in other prefibrillar amyloid species [33,39,41,42], we suggest that this conformational motif is central in the membrane-disruptive properties displayed by amyloid oligomers. In this context, it is worth noting that a porin-like structure was suggested for Aβ oligomers on the basis of striking spectral similarities between these species and the pore-forming OmpF porin [33]. Additionally, it has been shown that the A11 antibody recognizes amyloidogenic oligomers, as well as the pore-forming proteins α-haemolysin and human perforin [50], both of which self-assemble as β-barrels in biomembranes. Therefore, on the basis of the A11 reactivity (Figure 1) and our FTIR data (Figure 3), we hypothesize that the β-sheet-structured motif in AS oligomers might adopt a porin-like fold. In order to form such a supramolecular structure, each AS molecule would provide (at least) two β-strands that self-assemble as an antiparallel β-barrel which, although it spans the membrane, would place the unordered

regions towards one side of the bilayer. A cartoon representation of such an arrangement is included in Figure 4(C).

The various aspects of AS amyloid self-assembly and oligomer-induced toxicity discussed above are schematically depicted in Figure 4(C). Long-range interactions maintain the protein in its monomeric state. During self-assembly, antiparallel β-sheet-rich oligomers are formed, probably through intermolecular interactions mediated by regions enclosing β1 and β2. Oligomeric species are trapped by several small-molecule inhibitors that target the region near Tyr[39], preventing the structural reorganization required for fibril growth. Oligomers may compromise cell viability via protein–protein and/or protein–membrane interactions mediated by structurally distinct regions of AS.

In summary, although our approach using ATR–FTIR cannot compete with NMR determinations in terms of atomic-scale resolution, we were able to show for the first time that on-pathway AS oligomers adopt a distinct antiparallel β-sheet structure, a signature that might be shared by other amyloid oligomers, underlying their common membrane-disrupting pathogenic action. In addition, the unordered structure may be central in defining the AS oligomer interactome, leading to the impairment of essential cellular functions. Therefore our findings provide fundamental knowledge on the structural organization within AS oligomers important for the understanding of oligomer-induced toxicity and for the development of therapeutic agents.

AUTHOR CONTRIBUTION

M. Soledad Celej, Jean-Marie Ruysschaert and Vincent Raussens designed the research. M. Soledad Celej and Rabia Sarroukh performed the research. M. Soledad Celej, Rabia Sarroukh and Vincent Raussens analysed the results. M. Soledad Celej, Rabia Sarroukh, Erik Goormaghtigh, Gerardo D. Fidelio, Jean-Marie Ruysschaert and Vincent Raussens discussed the results and wrote the paper.

ACKNOWLEDGEMENTS

We thank Dr T.M. Jovin (Laboratory of Cellular Dynamics, Max Planck Institute for Biophysical Chemistry, Göttingen, Germany) for providing the pT7-7 plasmid encoding the AS protein, A. Valiente, G. Lamberto, Dr C. Fernandez and Dr C. Bertoncini for insightful discussions, Dr C. Nome for technical assistance on TEM imaging, G. Heim and Dr D. Riedel for providing TEM grids and discussion on electron micrographs.

FUNDING

This work was supported by the Secretaria de Ciencia y Técnica-Universidad Nacional de Córdoba (SECyT-UNC), Consejo Nacional de Investigaciones Científicas y Tecnológicas (CONICET) [grant number PIP 2011-2013 GI 11220100100012], Fundación Florencio Fiorini (year 2010), Alexander von Humboldt Foundation (equipment grant to M.S.C.), Fondo para la Investigación Científica y Tecnológica (FONCyT) [grant number PICT 34084 (to G.D.F.)] and Ministerio de Ciencia, Tecnología e Innovación Productiva-Fonds de la Recherche Scientifique (MINCyT-FNRS) [grant number BE0903 (to G.D.F. and E.G.)]. M.S.C. and G.D.F. are Researcher Career members of CONICET. V.R. and E.G. are Senior Research Associate and Research Director at the National Funds for Scientific Research (Belgium) respectively.

REFERENCES

1 Chiti, F. and Dobson, C. M. (2006) Protein misfolding, functional amyloid, and human disease. Annu. Rev. Biochem. **75**, 333–366
2 Olzscha, H., Schermann, S. M., Woerner, A. C., Pinkert, S., Hecht, M. H., Tartaglia, G. G., Vendruscolo, M., Hayer-Hartl, M., Hartl, F. U. and Vabulas, R. M. (2011) Amyloid-like aggregates sequester numerous metastable proteins with essential cellular functions. Cell **144**, 67–78
3 Morimoto, R. I. (2008) Proteotoxic stress and inducible chaperone networks in neurodegenerative disease and aging. Genes Dev. **22**, 1427–1438
4 Butterfield, S. M. and Lashuel, H. A. (2010) Amyloidogenic protein-membrane interactions: mechanistic insight from model systems. Angew. Chem. Int. Ed. Engl. **49**, 5628–5654
5 Bucciantini, M., Giannoni, E., Chiti, F., Baroni, F., Formigli, L., Zurdo, J., Taddei, N., Ramponi, G., Dobson, C. M. and Stefani, M. (2002) Inherent toxicity of aggregates implies a common mechanism for protein misfolding diseases. Nature **416**, 507–511
6 Glabe, C. G. (2008) Structural classification of toxic amyloid oligomers. J. Biol. Chem. **283**, 29639–29643
7 Bolognesi, B., Kumita, J. R., Barros, T. P., Esbjorner, E. K., Luheshi, L. M., Crowther, D. C., Wilson, M. R., Dobson, C. M., Favrin, G. and Yerbury, J. J. (2010) ANS binding reveals common features of cytotoxic amyloid species. ACS Chem. Biol. **5**, 735–740
8 Campioni, S., Mannini, B., Zampagni, M., Pensalfini, A., Parrini, C., Evangelisti, E., Relini, A., Stefani, M., Dobson, C. M., Cecchi, C. and Chiti, F. (2010) A causative link between the structure of aberrant protein oligomers and their toxicity. Nat. Chem. Biol. **6**, 140–147
9 Dauer, W. and Przedborski, S. (2003) Parkinson's disease: mechanisms and models. Neuron **39**, 889–909
10 Weinreb, P. H., Zhen, W., Poon, A. W., Conway, K. A. and Lansbury, Jr, P. T. (1996) NACP, a protein implicated in Alzheimer's disease and learning, is natively unfolded. Biochemistry **35**, 13709–13715
11 Bertoncini, C. W., Jung, Y. S., Fernandez, C. O., Hoyer, W., Griesinger, C., Jovin, T. M. and Zweckstetter, M. (2005) Release of long-range tertiary interactions potentiates aggregation of natively unstructured α-synuclein. Proc. Natl. Acad. Sci. U.S.A. **102**, 1430–1435
12 Serpell, L. C., Berriman, J., Jakes, R., Goedert, M. and Crowther, R. A. (2000) Fiber diffraction of synthetic α-synuclein filaments shows amyloid-like cross-β conformation. Proc. Natl. Acad. Sci. U.S.A. **97**, 4897–4902
13 Chen, M., Margittai, M., Chen, J. and Langen, R. (2007) Investigation of α-synuclein fibril structure by site-directed spin labeling. J. Biol. Chem. **282**, 24970–24979
14 Heise, H., Hoyer, W., Becker, S., Andronesi, O. C., Riedel, D. and Baldus, M. (2005) Molecular-level secondary structure, polymorphism, and dynamics of full-length α-synuclein fibrils studied by solid-state NMR. Proc. Natl. Acad. Sci. U.S.A. **102**, 15871–15876
15 Vilar, M., Chou, H. T., Luhrs, T., Maji, S. K., Riek-Loher, D., Verel, R., Manning, G., Stahlberg, H. and Riek, R. (2008) The fold of α-synuclein fibrils. Proc. Natl. Acad. Sci. U.S.A. **105**, 8637–8642
16 Wood, S. J., Wypych, J., Steavenson, S., Louis, J. C., Citron, M. and Biere, A. L. (1999) α-Synuclein fibrillogenesis is nucleation-dependent. Implications for the pathogenesis of Parkinson's disease. J. Biol. Chem. **274**, 19509–19512
17 Fink, A. L. (2006) The aggregation and fibrillation of α-synuclein. Acc. Chem. Res. **39**, 628–634
18 Volles, M. J., Lee, S. J., Rochet, J. C., Shtilerman, M. D., Ding, T. T., Kessler, J. C. and Lansbury, Jr, P. T. (2001) Vesicle permeabilization by protofibrillar α-synuclein: implications for the pathogenesis and treatment of Parkinson's disease. Biochemistry **40**, 7812–7819
19 Kayed, R., Sokolov, Y., Edmonds, B., McIntire, T. M., Milton, S. C., Hall, J. E. and Glabe, C. G. (2004) Permeabilization of lipid bilayers is a common conformation-dependent activity of soluble amyloid oligomers in protein misfolding diseases. J. Biol. Chem. **279**, 46363–46366
20 van Rooijen, B. D., Claessens, M. M. and Subramaniam, V. (2008) Membrane binding of oligomeric α-synuclein depends on bilayer charge and packing. FEBS Lett. **582**, 3788–3792
21 Kim, H. Y., Cho, M. K., Kumar, A., Maier, E., Siebenhaar, C., Becker, S., Fernandez, C. O., Lashuel, H. A., Benz, R., Lange, A. and Zweckstetter, M. (2009) Structural properties of pore-forming oligomers of α-synuclein. J. Am. Chem. Soc. **131**, 17482–17489
22 Kayed, R., Head, E., Thompson, J. L., McIntire, T. M., Milton, S. C., Cotman, C. W. and Glabe, C. G. (2003) Common structure of soluble amyloid oligomers implies common mechanism of pathogenesis. Science **300**, 486–489
23 Danzer, K. M., Haasen, D., Karow, A. R., Moussaud, S., Habeck, M., Giese, A., Kretzschmar, H., Hengerer, B. and Kostka, M. (2007) Different species of α-synuclein oligomers induce calcium influx and seeding. J. Neurosci. **27**, 9220–9232
24 Karpinar, D. P., Balija, M. B., Kugler, S., Opazo, F., Rezaei-Ghaleh, N., Wender, N., Kim, H. Y., Taschenberger, G., Falkenburger, B. H., Heise, H. et al. (2009) Pre-fibrillar α-synuclein variants with impaired β-structure increase neurotoxicity in Parkinson's disease models. EMBO J. **28**, 3256–3268
25 Winner, B., Jappelli, R., Maji, S. K., Desplats, P. A., Boyer, L., Aigner, S., Hetzer, C., Loher, T., Vilar, M., Campioni, S. et al. (2011) *In vivo* demonstration that α-synuclein oligomers are toxic. Proc. Natl. Acad. Sci. U.S.A. **108**, 4194–4199
26 Frost, B. and Diamond, M. I. (2010) Prion-like mechanisms in neurodegenerative diseases. Nat. Rev. Neurosci. **11**, 155–159
27 Lashuel, H. A., Petre, B. M., Wall, J., Simon, M., Nowak, R. J., Walz, T. and Lansbury, Jr, P. T. (2002) α-Synuclein, especially the Parkinson's disease-associated mutants, forms pore-like annular and tubular protofibrils. J. Mol. Biol. **322**, 1089–1102

28 Hong, D. P., Fink, A. L. and Uversky, V. N. (2008) Structural characteristics of α-synuclein oligomers stabilized by the flavonoid baicalein. J. Mol. Biol. **383**, 214–223
29 Kaylor, J., Bodner, N., Edridge, S., Yamin, G., Hong, D. P. and Fink, A. L. (2005) Characterization of oligomeric intermediates in α-synuclein fibrillation: FRET studies of Y125W/Y133F/Y136F α-synuclein. J. Mol. Biol. **353**, 357–372
30 van Rooijen, B. D., Claessens, M. M. and Subramaniam, V. (2009) Lipid bilayer disruption by oligomeric α-synuclein depends on bilayer charge and accessibility of the hydrophobic core. Biochim. Biophys. Acta **1788**, 1271–1278
31 Apetri, M. M., Maiti, N. C., Zagorski, M. G., Carey, P. R. and Anderson, V. E. (2006) Secondary structure of α-synuclein oligomers: characterization by Raman and atomic force microscopy. J. Mol. Biol. **355**, 63–71
32 van Rooijen, B. D., van Leijenhorst-Groener, K. A., Claessens, M. M. and Subramaniam, V. (2009) Tryptophan fluorescence reveals structural features of α-synuclein oligomers. J. Mol. Biol. **394**, 826–833
33 Cerf, E., Sarroukh, R., Tamamizu-Kato, S., Breydo, L., Derclaye, S., Dufrene, Y. F., Narayanaswami, V., Goormaghtigh, E., Ruysschaert, J. M. and Raussens, V. (2009) Antiparallel β-sheet: a signature structure of the oligomeric amyloid β-peptide. Biochem. J. **421**, 415–423
34 Celej, M. S., Jares-Erijman, E. A. and Jovin, T. M. (2008) Fluorescent N-arylamino-naphthalene sulfonate probes for amyloid aggregation of α-synuclein. Biophys. J. **94**, 4867–4879
35 Goormaghtigh, E., Cabiaux, V. and Ruysschaert, J. M. (1994) Determination of soluble and membrane protein structure by Fourier transform infrared spectroscopy. I. Assignments and model compounds. Subcell. Biochem. **23**, 329–362
36 Oberg, K. A., Ruysschaert, J. M. and Goormaghtigh, E. (2003) Rationally selected basis proteins: a new approach to selecting proteins for spectroscopic secondary structure analysis. Protein Sci. **12**, 2015–2031
37 Chirgadze, Y. N. and Nevskaya, N. A. (1976) Infrared spectra and resonance interaction of amide-I vibration of the parallel-chain pleated sheets. Biopolymers **15**, 627–636
38 Chirgadze, Y. N. and Nevskaya, N. A. (1976) Infrared spectra and resonance interaction of amide-I vibration of the antiparallel-chain pleated sheet. Biopolymers **15**, 607–625
39 Habicht, G., Haupt, C., Friedrich, R. P., Hortschansky, P., Sachse, C., Meinhardt, J., Wieligmann, K., Gellermann, G. P., Brodhun, M., Gotz, J. et al. (2007) Directed selection of a conformational antibody domain that prevents mature amyloid fibril formation by stabilizing Aβ protofibrils. Proc. Natl. Acad. Sci. U.S.A. **104**, 19232–19237
40 Sarroukh, R., Cerf, E., Derclaye, S., Dufrene, Y. F., Goormaghtigh, E., Ruysschaert, J. M. and Raussens, V. (2011) Transformation of amyloid β(1–40) oligomers into fibrils is characterized by a major change in secondary structure. Cell. Mol. Life Sci. **68**, 1429–1438
41 Natalello, A., Prokorov, V. V., Tagliavini, F., Morbin, M., Forloni, G., Beeg, M., Manzoni, C., Colombo, L., Gobbi, M., Salmona, M. and Doglia, S. M. (2008) Conformational plasticity of the Gerstmann-Straussler-Scheinker disease peptide as indicated by its multiple aggregation pathways. J. Mol. Biol. **381**, 1349–1361
42 Fabian, H., Gast, K., Laue, M., Misselwitz, R., Uchanska-Ziegler, B., Ziegler, A. and Naumann, D. (2008) Early stages of misfolding and association of β2-microglobulin: insights from infrared spectroscopy and dynamic light scattering. Biochemistry **47**, 6895–6906
43 Suk, J. E., Lokappa, S. B. and Ulmer, T. S. (2010) The clustering and spatial arrangement of β-sheet sequence, but not order, govern α-synuclein fibrillogenesis. Biochemistry **49**, 1533–1540
44 Tartaglia, G. G., Pawar, A. P., Campioni, S., Dobson, C. M., Chiti, F. and Vendruscolo, M. (2008) Prediction of aggregation-prone regions in structured proteins. J. Mol. Biol. **380**, 425–436
45 Giasson, B. I., Murray, I. V., Trojanowski, J. Q. and Lee, V. M. (2001) A hydrophobic stretch of 12 amino acid residues in the middle of α-synuclein is essential for filament assembly. J. Biol. Chem. **276**, 2380–2386
46 Rao, J. N., Dua, V. and Ulmer, T. S. (2008) Characterization of α-synuclein interactions with selected aggregation-inhibiting small molecules. Biochemistry **47**, 4651–4656
47 Meng, X., Munishkina, L. A., Fink, A. L. and Uversky, V. N. (2009) Molecular mechanisms underlying the flavonoid-induced inhibition of α-synuclein fibrillation. Biochemistry **48**, 8206–8224
48 Lamberto, G. R., Binolfi, A., Orcellet, M. L., Bertoncini, C. W., Zweckstetter, M., Griesinger, C. and Fernandez, C. O. (2009) Structural and mechanistic basis behind the inhibitory interaction of PcTS on α-synuclein amyloid fibril formation. Proc. Natl. Acad. Sci. U.S.A. **106**, 21057–21062
49 Dusa, A., Kaylor, J., Edridge, S., Bodner, N., Hong, D. P. and Fink, A. L. (2006) Characterization of oligomers during α-synuclein aggregation using intrinsic tryptophan fluorescence. Biochemistry **45**, 2752–2760
50 Yoshiike, Y., Kayed, R., Milton, S. C., Takashima, A. and Glabe, C. G. (2007) Pore-forming proteins share structural and functional homology with amyloid oligomers. NeuroMol. Med. **9**, 270–275

Received 28 October 2011/30 January 2012; accepted 8 February 2012
Published as BJ Immediate Publication 8 February 2012, doi:10.1042/BJ20111924